International Journal of New Technology and Research (IJNTR)
ISSN:2454-4116, Volume-4, Issue-6, June 2018 Pages 10-15

A Numerical Study of the SVC-Controlled Electric Power System Dynamics

Der-Cherng Liaw, Jun-Wei Chen, Yun-Hua Huang

***Abstract*—A numerical study of nonlinear dynamics for electric power system with the Static Var Compensator (SVC) control is presented in this paper. In the previous design (Liaw et al, 2009), we have proposed A sliding mode control (SMC) based output tracking scheme for regulating the load voltage of the electric power system. In this paper, we will extend the previous design to consider the effect of the load variation. The relationship between the time constant of SVC controller and the changing rate of load variation is obtained by using numerical study, which will then guarantee the success of the voltage tracking design with respect to the variation of both reactive power and real power.**

***Index Terms*—power system, stability, control, load**

I. Introduction

The study of voltage collapse in the electric power systems has recently attracted lots of attention (e.g., [1]-[4]), which is mainly due to the fact of facing the growing load demands in power systems but with little addition of the power generation and transmission facilities. It is known that the power systems will be operated near the stability limits and make the magnitude of load voltage falls sharply to a very low level as the load demands become too heavy to be offered. Such a phenomenon is referred as the so-called "voltage collapse." A practical power system is a large electric network containing components such as generators, loads, transmission lines and voltage controllers. In 1988, Dobson and Chiang introduced a simple dynamical model for electric power systems, which consist of a generator, a nonlinear load and an infinite bus [1]. Based on that model, several results have been published regarding the nonlinear phenomena of electric power systems (e.g., [1]-[2]). Among those results, the occurrence of voltage collapse had been believed to be attributed to the existence of saddle-node bifurcation of electric power systems [2] and/or the existence of Hopf bifurcation which is prior to the appearance of saddle-node bifurcation [3]. In addition, it is known that the voltage regulation issue can be solved by the setting of the tap changing ratio (e.g., [4]-[5]) or the extra adding capacitive load in practical electric power systems. However, both schemes are only available for discrete tuning. The Static Var Compensator (SVC) has recently been considered as a control actuator for improving system stability (e.g., [6]-[7]). Instead of directly controlling the system behavior at the bifurcation point as proposed in [6], in [7] we have proposed a load voltage regulation design via the tuning of the SVC. Such a design is based on the sliding mode control scheme, which might also eliminate and/or delay the occurrence of bifurcation phenomena and system instabilities. In this paper, we continue the study of [7] by considering the PQ-load is a time-variant input. Numerical simulation will be carried on to study the effectiveness of the previous proposed design in delaying the occurrence of the system instabilities even with time-variant power load.

The organization of the paper is given as follows. First, the mathematical model of electric power system and the output tracking control scheme proposed in [7] are both recalled in Section 2. It is followed by numerical study of the dynamical behavior of electric power system with respect to the variation of power load and system design parameters. Finally, Section 4 gives the conclusions.

II. Preliminaries

In this section, we will first recall the mathematical model proposed by Dobson and Chiang [1] for electric power systems. It is followed by the recall of the load voltage tracking design [7] for the power system via the tuning of the SVC controller.

A. Power System Model

In the following, we recall the mathematical model proposed by Dobson and Chiang [1] for electric power systems as given by

$$\dot{\delta}_m = \omega_m, \tag{1}$$

$$M\dot{\omega}_m = P_m - d_m\omega_m + E_m^2 Y_m \sin\theta_m + E_m Y_m V \sin(\delta - \delta_m - \theta_m), \tag{2}$$

$$k_{qw}\dot{\delta} = -k_{qv2}V^2 - k_{qv}V + Q(\delta_m, \delta, V) - Q_0 - Q_1, \tag{3}$$

$$Tk_{qw}k_{pv}\dot{V} = k_{p\omega}k_{qv^2}V^2 + (k_{p\omega}k_{qv} - k_{q\omega}k_{pv})V + k_{q\omega}(P(\delta_m, \delta, V) - P_0 - P_1) - k_{p\omega}(Q(\delta_m, \delta, V) - Q_0 - Q_1), \tag{4}$$

where δ_m, ω_m, δ and V denote the generator phase angle, generator angular speed, load voltage phase angle and load voltage, respectively. In addition, the nonlinear PQ load are given as

Der-Cherng Liaw, Institute of Electrical Control Engineering, National Chiao Tung University, 1001 Ta Hsueh Road, Hsinchu, Taiwan, R.O.C.
Jun-Wei Chen, Institute of Electrical Control Engineering, National Chiao Tung University, 1001 Ta Hsueh Road, Hsinchu, Taiwan, R.O.C.
Yun-Hua Huang, Institute of Electrical Control Engineering, National Chiao Tung University, 1001 Ta Hsueh Road, Hsinchu, Taiwan, R.O.C.

$$P(\delta_m,\delta,V) = (Y_0'\sin\theta_0' + Y_m\sin\theta_m)V^2 - E_mY_mV\sin(\delta-\delta_m+\theta_m) - E_0'Y_0'V\sin(\delta+\theta_0'),$$

$$Q(\delta_m,\delta,V) = -(Y_0'\cos\theta_0' + Y_m\cos\theta_m)V^2 + E_mY_mV\cos(\delta-\delta_m+\theta_m) + E_0'Y_0'V\cos(\delta+\theta_0'),$$

with

$$E_0' = E_0[1+C^2Y_0^{-2}-2CY_0^{-1}\cos\theta_0]^{-1/2},$$
$$Y_0' = Y_0[1+C^2Y_0^{-2}-2CY_0^{-1}\cos\theta_0]^{1/2},$$
$$\theta_0' = \theta_0 + \tan^{-1}\left\{\frac{CY_0^{-1}\sin\theta_0}{1-CY_0^{-1}\cos\theta_0}\right\}.$$

For details, the definitions of each system parameter and derivations of the model equations above can be referred to [1].

B. SVC-controlled system via SMC approach

In the recent years, the SVC's have been considered as a control scheme for voltage regulation in the electric power systems. The configuration of the SVC provides an additional reactive power when it is connected in parallel with the PQ load. That is, the overall effective reactive load Q_1 will become the summation of the original demanded reactive load Q_1^0 and the added reactive load Q_1^{added} from the SVC's. The mathematical model of the SVC's has been proposed (e.g., [6]) as given by

$$\dot{B} = \frac{1}{T_{SVC}}\left(K_{SVC}\cdot u - B\right),$$

with $B_{\min} \le B \le B_{\max}$. Here, B denotes the susceptance of the SVC, K_{SVC} is the gain for the SVC, T_{SVC} denotes the time constant and u denotes the control input. In addition, the added reactive load by the SVC's is given as $Q_1^{added} = BV^2$.

Let $x = [x_1 \quad x_2 \quad x_3 \quad x_4]^T$ and $x_5 = B$, where $x_1 = \delta_m$, $x_2 = \omega_m$, $x_3 = \delta$, and $x_4 = V$. Then we can rewrite system (1)-(4) with SVC control as follows:

$$\dot{x}_1 = x_2, \tag{5}$$

$$\dot{x}_2 = \frac{1}{M}\{P_m - d_m x_2 + E_m^2 Y_m\sin\theta_m + E_mY_mx_4\sin(x_3-x_1-\theta_m)\}, \tag{6}$$

$$\dot{x}_3 = \frac{1}{k_{qw}}\{-k_{qv2}x_4^2 - k_{qv}x_4 + Q(x_1,x_3,x_4) - Q_0 - Q_1 - x_5x_4^2\}, \tag{7}$$

$$\dot{x}_4 = \frac{1}{Tk_{qw}k_{pv}}\{k_{p\omega}k_{qv2}x_4^2 + (k_{p\omega}k_{qv} - k_{q\omega}k_{pv})x_4 + k_{q\omega}(P(x_1,x_3,x_4) - P_0 - P_1) - k_{p\omega}(Q(x_1,x_3,x_4) - Q_0 - Q_1 - x_5x_4^2)\}, \tag{8}$$

$$\dot{x}_5 = \frac{1}{T_{SVC}}\left(K_{SVC}\cdot u - x_5\right), \tag{9}$$

where the extra demanded reactive load has become $Q_1 + x_5x_4^2$ with Q_1 denotes the original demanded reactive load and $x_5x_4^2$ is for the added reactive load created by the SVC's. In the design of [7], $V_d(t)$ denotes the desired load voltage for system (5)-(9). The result for the load voltage tracking control of system (5)-(9) is recalled from [7] as given in the next theorem.

Theorem 1: The load voltage V denoted as x_4 of system (5)-(9) will approach the desired voltage $V_d(t)$ via sliding mode control if $K_{SVC}/T_{SVC} \neq 0$ and $(k_{p\omega}/Tk_{q\omega}k_{pv})\cdot x_4^2 \neq 0$. Moreover, one of the choices for the control input u can be given as that in (10) below with $y_d = V_d(t)$:

$$u = \frac{T_{SVC}}{K_{SVC}}\{\dot{\phi}(x,y_d) - \beta\cdot\mathrm{sgn}(s) + \frac{1}{T_{SVC}}\cdot x_5\} \tag{10}$$

where

$$\phi(x,y_d) = \frac{Tk_{qw}k_{pv}}{k_{p\omega}x_4^2}\cdot[-h(x) + \dot{y}_d - (x_4 - y_d)]$$
$$s = x_5 - \phi(x,y_d)$$

with

$$h(x) = \frac{1}{Tk_{qw}k_{pv}}\{k_{p\omega}k_{qv^2}x_4^2 + (k_{p\omega}k_{qv} - k_{q\omega}k_{pv})x_4 + k_{q\omega}(P(x_1,x_3,x_4) - P_0 - P_1) - k_{p\omega}(Q(x_1,x_3,x_4) - Q_0 - Q_1)\}.$$

Based on the design of the Theorem 1 above, numerical simulations have been given in [7] to demonstrate the success of the proposed design for the static setting of the extra reactive load.

III. Main Results

Instead of letting the extra reactive load be a fixed value, in the following we will not only consider the extra PQ-load is a time-variant function but also study the effect of the control parameters of the SVC actuator on system performance.

A. Open-Loop Dynamics with Different Static Load

First, we present the numerical results for the uncontrolled system (1)-(4) with respect to the variation of PQ-load. Here, we adopt the value of system parameters as given in TABLE I for system (1)-(4) from [7]. Bifurcation diagrams of the load voltage (denoted as x_4) with respect to the different setting of extra PQ-load are obtained by using code AUTO [8] as depicted in Fig. 1, where the solid-line denotes the stable system equilibria and the dashed-dot-line is for the unstable ones. Figure 1 shows that there are both Hopf bifurcation and saddle-node bifurcation for $P_1 \le 0.1513$, respectively, as denoted by "HB" and "SNB". However, there is only a saddle-node bifurcation for $P_1 > 0.1514$. The values of Q_1 at HB and SNB for each value of P_1 are also listed in TABLE II. The symbol '-' in TABLE II denotes that the HB does not exist. When P_1 is increasing from 0 to 0.2, the values of Q_1 at SNB are found to be increasing. However, the values of Q_1 at SNB are decreasing for $P_1 > 0.2$. Time responses of load voltage x_4 with respect to different values of P_1 and Q_1 are shown in Figs. 2-4. It is observed from Figs. 2-3 that the load

voltage x_4 will approach to a stable and steady value at $Q_1 = 2.5$ and $Q_1 = 2.7$ for $P_1 \le 1$. However, the load voltage x_4 will be collapsed at for Q_1 =2.9802183287 with $P_1 = 1$ as depicted in Fig. 4(d). Those time responses agree with the bifurcation diagram as shown in Fig.1.

TABLE I. Data for system parameters

$K_{p\omega} = 0.4$ p.u.	$K_{pv} = 0.3$ p.u.	$K_{q\omega} = -0.003$ p.u.
$K_{qv} = -2.8$ p.u.	$K_{qv2} = 2.1$ p.u.	$T = 8.5$ p.u.
$P_0 = 0.6$ p.u.	$Q_0 = 1.3$ p.u.	$M = 0.01464$
$Y_0 = 3.33$ p.u.	$\theta_0 = 0$ deg.	$E_0 = 1.0$ p.u.
$C = 3.5$ p.u	$Y_m = 5.0$ p.u.	$\theta_m = 0$ deg.
$E_m = 1.05$ p.u.	$P_m = 1.0$ p.u.	$d_m = 0.05$ p.u.

TABLE II. Location of bifurcation points

P_1	Q_1 at HB	Q_1 at SNB
0	2.9802183287	3.0257810507
0.1	3.023875938	3.0300035165
0.1513	3.030702709	3.0307060238
0.1514	-	3.0307064235
0.2	-	3.030453767
0.5	-	3.0090175864
1.0	-	2.8945266365
1.5	-	2.6708492979
2.0	-	2.314373463
2.5	-	1.7841152012
3.0	-	1.0209601514
3.2	-	0.63602092587
3.45	-	0.082890487695

B. Effects of Control parameters

Next, we consider the effect of the SVC controller on the system performance. In [7], we chose $y_d = V_d(t) = 1$ as the desired target for voltage regulation. Here, we continue the study of [7] with the same objective. As shown in Fig. 5, the tracking performance of power system are observed to be the same disregard the values of the time constant T_{SVC} and the control gain K_{SVC} of the SVC control given in (9). In fact, after carefully checking the dynamical behavior of the SVC control as given in Eq. (9) can be rewritten as

$$\dot{x}_5 = \frac{1}{T_{SVC}}(K_{SVC} \cdot u - x_5) = \dot{\phi} - \beta \cdot \mathrm{sgn}(s).$$

That means the control performance will depend on the choice of control gain β only, which has no relationship with the value of T_{SVC} or K_{SVC}. In the following numerical study, we choose $T_{SVC} = 10$ and $K_{SVC} = 10$. Time responses of load voltage tracking for $Q_1 = 2.9802183287$ and $Q_1 = 3$ with $\beta = 2,\ 10$ and 100 are shown in Figs. 6-7, respectively. It is clear to see that the tracking performance becomes better as the value of β increases. The tracking performance with respect to the different setting value of β is also shown in Fig. 8.

C. Effects of Control parameters

Now, we consider the PQ-load is a time-variant function by letting $Q_1 = 2.9802183287 + 0.7\sin(2\pi t / T_Q)$ near the Hopf bifurcation point as depicted in Fig. 9 for $T_Q = 10,\ 100$ and 1000. Time responses of load voltage tracking for $Q_1 = 2.9802183287$ and $Q_1 = 3$ with $T_Q = 10,\ 100$ and 1000, $\beta = 2$ and 100, and $P_1 = 0,\ 0.1,\ 0.2$ are shown in Figs. 10-27. It is observed from those simulations that the tracking control might be fail when the period T_Q is small with small value of β disregard the values of P_1 or Q_1. Instead, the tracking design can be workable for small T_Q only if the value of β is big enough.

IV. Conclusion

A numerical study of control performance for SVC-based load voltage tracking is presented in the paper. It is found that the tracking performance of the proposed scheme in [7] depends on the control parameter of the reaching condition in sliding mode design. In addition, the proposed tracking design might be fail when the period T_Q of load variation is too small if the control parameter β is not big enough. Those results might provide a guide in the practical application.

References

[1] I. Dobson, H.-D. Chiang, J. S. Throp and L. Fekih-Ahmed, "A model of voltage collapse in electric power systems," *Proc. 27th IEEE Conference on Decision and Control*, Austin, Texas, pp. 2104-2109, Dec. 1988.

[2] H.-D. Chiang, I. Dobson, R. J. Thomas, J. S. Throp and L. Fekih-Ahmed, "On voltage collapse in electric power systems," *IEEE transactions on Power Systems*, vol. 5, no. 2, pp. 601-611, 1990.

[3] H. O. Wang, E. H. Abed, and A. M. A. Hamdan, "Bifurcations, chaos, and crises in voltage collapse of a model power system," *IEEE Transactions on Circuits and Systems–I: Fundamental Theory and Applications*, vol. 41, no. 3, pp. 294-302, 1994.

[4] C.-C. Liu and K. T. Vu, "Analysis of tap-changer dynamics and construction of voltage stability regions," *IEEE Transactions on Circuits and Systems*, vol. 36, no. 4, pp. 575-589, 1989.

[5] D.-C. Liaw, K.-H. Fang and C.-C. Song, "Bifurcation Analysis of Power Systems with Tap Changer," *Proc. 2005 IEEE International Conference on Networking, Sensing and Control (ICNSC'05)*, Tucson, Arizona, U.S.A., March 19-22, 2005.

[6] M. S. Saad, M. A. Hassouneh, E. H. Abed, and A. Edris, "Delaying instability and voltage collapse in power systems using svc's with washout filter-aided feedback," *Proc. 2005 American Control Conf., Portland*, June 8-10, 2005.

[7] D.-C Liaw, S.-T Chang, and Y.-H Huang, "Voltage tracking design for electric power systems via SMC approach," *Proc. 48th IEEE Conference on Decision and Control, 28th Chinese Control Conference (CDC/CCC '09)*, Shanghai, China, Dec. 2009.

[8] E. Doedel, AUTO 86 User Manual, Computer Science Dept., Soncordia Univ., Jan. 1986.

Der-Cherng Liaw Institute of Electrical Control Engineering, National Chiao Tung University, Hsinchu, Taiwan, R.O.C.

Jun-Wei Chen Institute of Electrical Control Engineering, National Chiao Tung University, Hsinchu, Taiwan, R.O.C.

Yun-Hua Huang Institute of Electrical Control Engineering, National Chiao Tung University, Hsinchu, Taiwan, R.O.C.

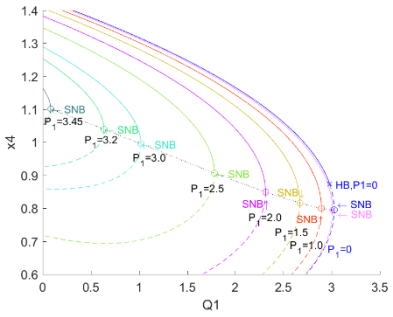

Fig. 1 Bifurcation diagram x_4 with respect to P_1 and Q_1

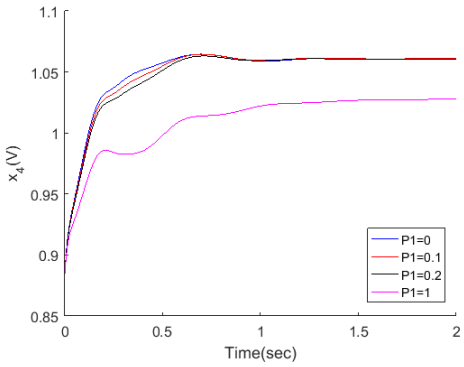

Fig. 2 Open loop time response of state x_4 for Q_1 =2.5.

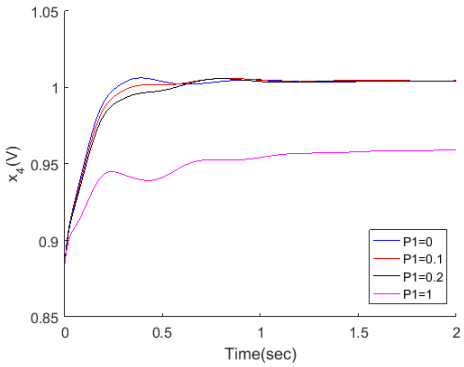

Fig. 3 Open loop time response of state x_4 for Q_1 =2.7.

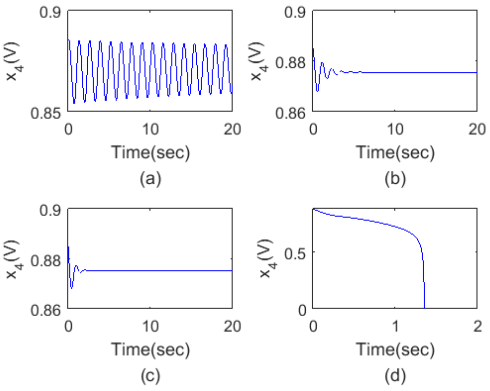

Fig. 4 Open loop time response of state x_4 for Q_1 =2.9802183287: (a) P_1 =0, (b) P_1 =0.1, (c) P_1 =0.2, and (d) P_1 =1.

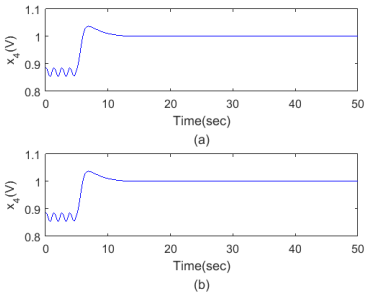

Fig. 5 Time response of state x_4 applied control at t =5 with β =1: (a) T_{SVC} =0.1 and K_{SVC} =0.1. (b) T_{SVC} =10 and K_{SVC} =10.

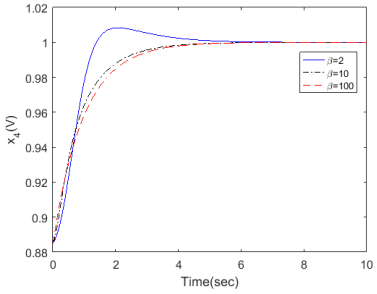

Fig. 6 Time response of state x_4 for Q_1 =2.9802183287 with β =2, 10 and 100.

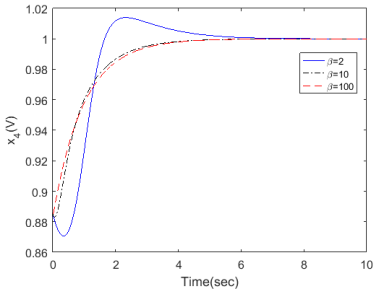

Fig. 7 Time response of state x_4 for Q_1 =3 with β =2, 10 and 100.

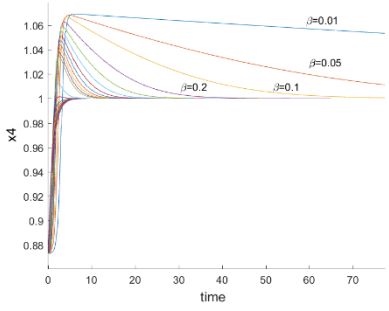

Fig. 8 The tracking performance for β =0.01 to 1000

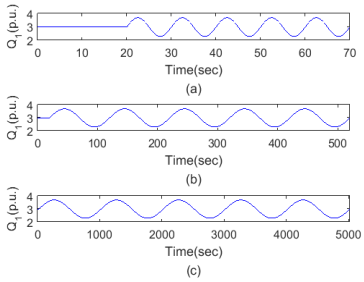

Fig. 9 Reactive load Q_1 for different T_Q :(a) T_Q =10, (b) T_Q =100, and (c) T_Q =1000.

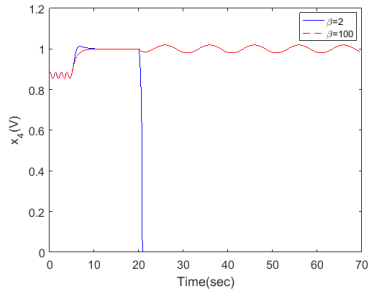

Fig. 10 The tracking performance for T_Q =10 with β = 2 and 100 for Q_1 =2.9802183287 and P_1 =0.

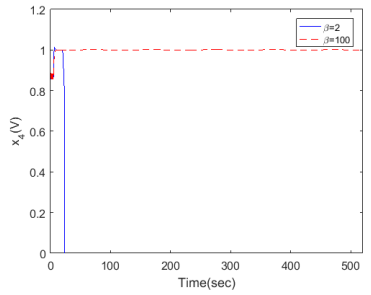

Fig. 11 The tracking performance for T_Q =100 with β = 2 and 100 for Q_1 =2.9802183287 and P_1 =0.

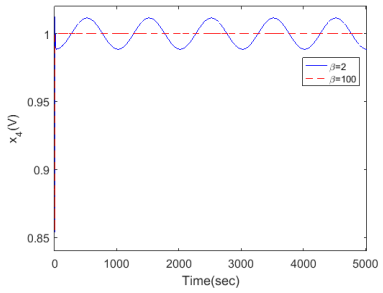

Fig. 12 The tracking performance for T_Q =1000 with β = 2 and 100 for Q_1 =2.9802183287 and P_1 =0.

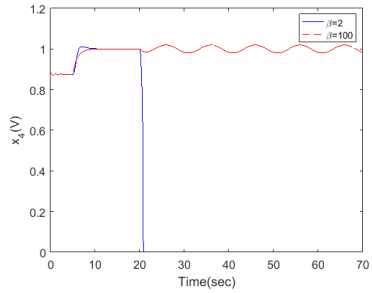

Fig. 13 The tracking performance for T_Q =10 with β = 2 and 100 for Q_1 =2.9802183287 and P_1 =0.1.

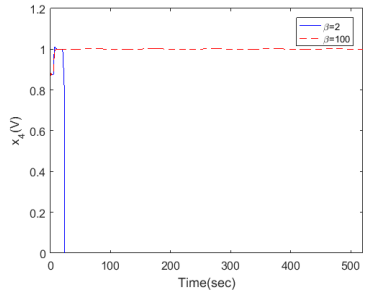

Fig. 14 The tracking performance for T_Q =100 with β = 2 and 100 for Q_1 =2.9802183287 and P_1 =0.1.

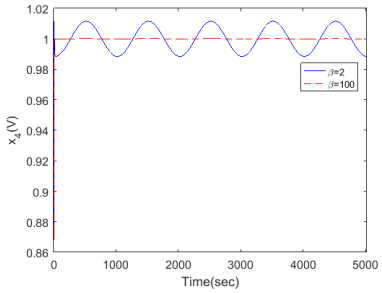

Fig. 15 The tracking performance for T_Q =1000 with β = 2 and 100 for Q_1 =2.9802183287 and P_1 =0.1.

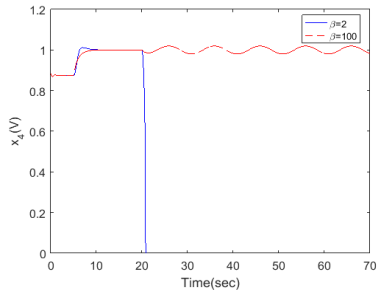

Fig. 16 The tracking performance for T_Q =10 with β = 2 and 100 for Q_1 =2.9802183287 and P_1 =0.2.

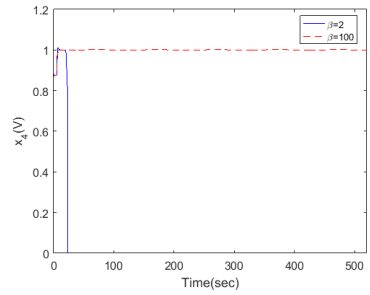

Fig. 17 The tracking performance for T_Q =100 with β = 2 and 100 for Q_1 =2.9802183287 and P_1 =0.2.

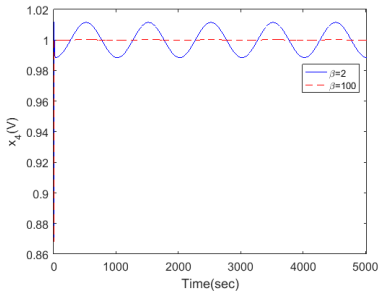

Fig. 18 The tracking performance for T_Q =1000 with β = 2 and 100 for Q_1 =2.9802183287 and P_1 =0.2.

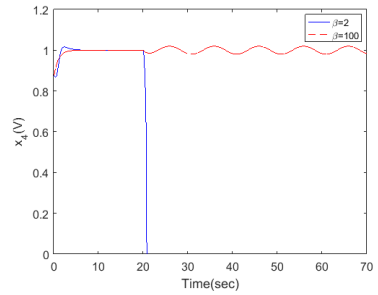

Fig. 19 The tracking performance for T_Q =10 with β = 2 and 100 for Q_1 =3 and P_1 =0.

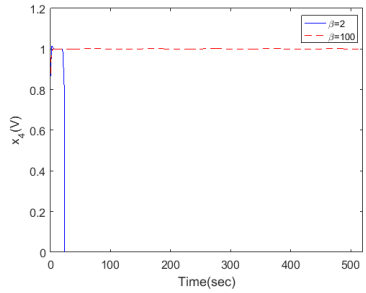

Fig. 20 The tracking performance for T_Q =100 with β = 2 and 100 for Q_1 =3 and P_1 =0.

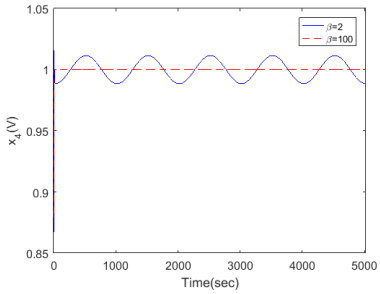

Fig. 21 The tracking performance for T_Q =1000 with β = 2 and 100 for Q_1 =3 and P_1 =0.

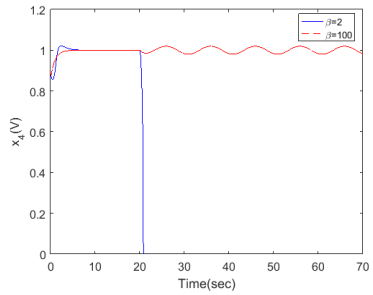

Fig. 22 The tracking performance for T_Q =10 with β = 2 and 100 for Q_1 =3 and P_1 =0.1.

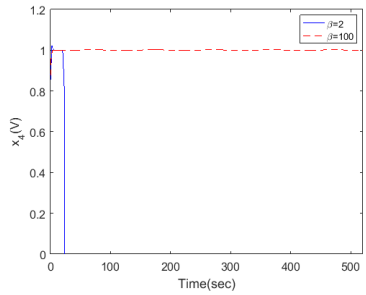

Fig. 23 The tracking performance for T_Q =100 with β = 2 and 100 for Q_1 =3 and P_1 =0.1.

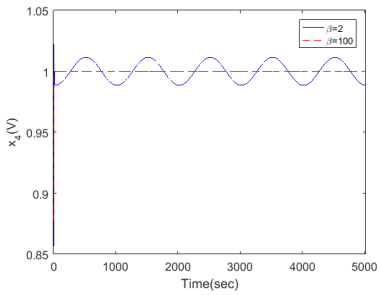

Fig. 24 The tracking performance for T_Q =1000 with β = 2, and 100 at Q_1 =3 and P_1 =0.1.

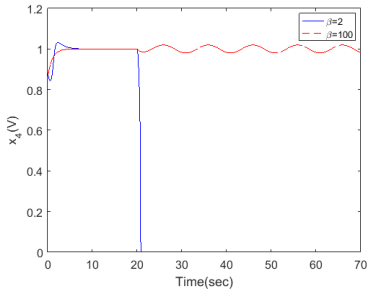

Fig. 25 The tracking performance for T_Q =10 with β = 2 and 100 for Q_1 =3 and P_1 =0.2.

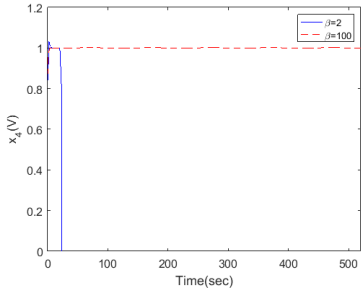

Fig. 26 The tracking performance for T_Q =100 with β = 2 and 100 for Q_1 =3 and P_1 =0.2.

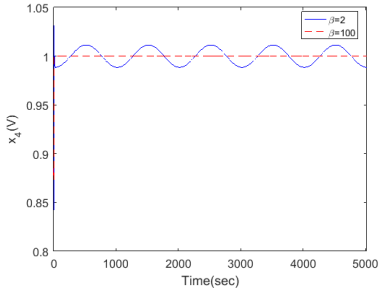

Fig. 27 The tracking performance for T_Q =1000 with β = 2 and 100 for Q_1 =3 and P_1 =0.2.